Vibrational Analysis of Peptides, Polypeptides, and Proteins. XXXII. α-Poly(L-Glutamic Acid)

PRADEEP K. SENGUPTA and S. KRIMM, *Biophysics Research Division, University of Michigan, Ann Arbor, Michigan 48109*

Synopsis

The Raman and ir spectra of α-helical poly(L-glutamic acid) have been assigned on the basis of a normal mode calculation for this structure. The force field was based on our previously refined main-chain force constants for α-poly(L-alanine) and side-chain force constants for β-calcium–poly(L-glutamate). Despite the identical backbone α-helical structures, significantly different frequencies are calculated, and observed, in the amide III and backbone stretch regions of α-poly(L-glutamic acid), as compared with α-poly(L-alanine). This clearly demonstrates the influence of side-chain structure on main-chain vibrational modes.

INTRODUCTION

In a previous paper,[1] we presented an analysis of the Raman and ir spectra of calcium poly(L-glutamate) [(GluCa)$_n$] in the β-sheet conformation, based on normal mode calculations of the antiparallel-chain pleated-sheet structure. In this paper, we analyze the vibrational spectra of the α-helix conformation of this polypeptide, particularly in the acid form, viz., poly(L-glutamic acid) [(GluH)$_n$], again with the aid of normal mode calculations. Such calculations provide the most powerful method of correlating the vibrational spectrum with the conformation of a polypeptide chain.[2] The results of this analysis not only help to interpret the Raman and ir spectra of α-(GluH)$_n$, but they show how the chemical composition of the side chain influences the vibrations of the main chain. They also provide a basis for analyzing the conformation of the charged form of (GluH)$_n$ (P. K. Sengupta and S. Krimm, to be published).

The α-(GluH)$_n$ conformation has been studied by ir and Raman techniques, both in the solid state[3-8] and in solution.[9,10] The existence of a folded structure was first proposed by Ambrose[3] on the basis of ir dichroism measurements on solid films cast from solutions in dimethylformamide (DMF). One of the motivations for that study was to compare the structure of the synthetic polypeptide with that of the poly(D-glutamic acid) isolated from *Bacillus anthracis*. It was found that, while the synthetic material was exclusively in the α-helix conformation, the natural polypeptide consisted of a mixture of α-helix and β-sheet conformations. Subsequent studies of the vibrational spec-

tra of $(GluH)_n$ were related to the helix–coil transition of this poly-peptide and its relevance to the processes of protein denaturation. These studies confirmed that $(GluH)_n$ adopts an α-helix conformation in the solid state and in aqueous solutions at low pH, i.e., under conditions where the COOH groups are nonionized. Recent Raman studies on $(GluCa)_n$ in the hexagonal crystalline form[11] have indicated that both of these salts also adopt α-helix conformations in the dry state.

While previous studies have focussed on the interpretation of isolated features of the ir and Raman spectra, we present here a detailed analysis based on a normal mode calculation of the α-helix structure.

MATERIALS AND METHODS

The $(GluH)_n$ sample used in this study was obtained from Miles Laboratories, Inc. (Lot No. 802, $M = 63,800$). For the ir measurements, films were cast from a DMF solution on to AgBr plates. A partially N-deuterated sample was prepared as follows: D_2O was added to a solution of $(GluH)_n$ in DMF. This was allowed to sit for several hours, after which the solvent was evaporated in a vacuum oven at room temperature. This sample was redissolved in DMF and the above procedure repeated two more times.

Most of the ir measurements were made at 2 cm^{-1} resolution on a Digilab FTS-20C Fourier transform ir spectrometer, with some measurements made on a Nicolet 60SX instrument. The common frequencies are in reasonably good agreement with literature values; we also present additional data in the NH and CH stretch regions, and weak bands in the 1800–400-cm^{-1} region not listed by previous workers. The Raman data used in this study were taken from Fasman, et al.,[8] with the exception of the CH_2 stretch region, which was measured in this laboratory using a Raman spectrometer described previously.[1]

NORMAL MODE CALCULATIONS

The normal mode calculation was done on an α-helix conformation identical to that of α-$(Ala)_n$,[12] i.e., with helix parameters of $n = 3.62$, $h = 1.495$ Å, and t (rotation per residue) $= 99.57°$, leading to dihedral angles of $\phi = -57.37°$ and $\psi = -47.49°$. The side chains were assumed to be fully extended, and their dihedral angles were taken from the comparable structure in β-$(GluCa)_n$.[1] For convenience, the COOH group was replaced by a COO$^-$ group; this should have a small effect on the main-chain modes, but may influence some side-chain frequencies. (We will identify specific COOH bands in the spectra.) The internal and local symmetry coordinates were defined as before,[1] except that in the present case we do not require the $H^{\alpha} \cdots H^{\alpha}$ stretching coordinate.

The vibrationally active modes of the α-helix are classified into A(δ = 0°), E_1(δ = 99.57°), and E_2(δ = 199.04°) symmetry species, where δ is the phase difference between the motions in adjacent residues. The A and E_1 species modes are both ir and Raman active and have parallel and perpendicular ir dichroism, respectively. The E_2 species modes are Raman active only. For our structure, there are 43 A, 44 E_1, and 45 E_2 modes.

The force constants for the main chain and those involving the coupling of the C^β atom to the backbone were taken from the work on α-(Ala)$_n$.[12] The force constants for the side chain were transferred from β-(GluCa)$_n$.[1] As in the previous calculation for the α-helix,[12] transition dipole coupling was included for amide I and amide II modes, leading to calculated splittings identical to those for α-(Ala)$_n$.

RESULTS AND DISCUSSION

The ir spectra of a solid film of α-(GluH)$_n$ are given in Figs. 1 and 2A, with the spectrum of a partially N-deuterated sample being given in Fig. 2B. The observed Raman[8] and ir bands, together with the calculated frequencies and their potential energy distributions (PED), are given in Table I.

The amide A mode, which is NH stretch perturbed by Fermi resonance, is observed at 3301 cm^{-1}, close to the value of 3307 cm^{-1} found in α-(Ala)$_n$.[13] (We must point out that the OH stretch mode of the
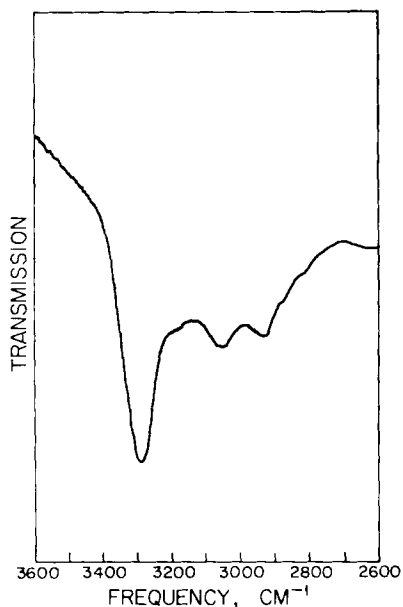

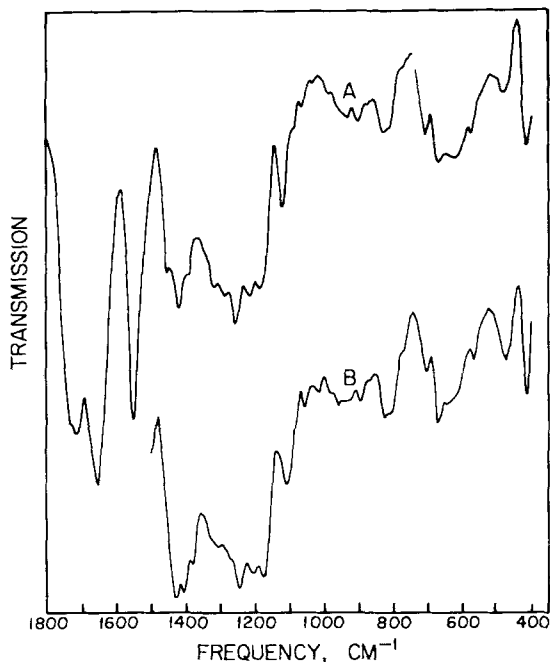Fig. 1. The ir spectrum of α-poly(L-glutamic acid) in the 2600–3600-cm^{-1} region.

Fig. 2. The ir spectrum of α-poly(L-glutamic acid) in the 400–1800-cm^{-1} region: (A) parent compound, (B) partially N-deuterated derivative.

COOH group is expected in the same general region as NH stretch, but no conspicuous sharp band is observed that can be readily assigned to this mode.) The amide B mode, which is the other component of the Fermi resonance doublet, is observed at 3067 cm^{-1}, compared with 3058 cm^{-1} in α-(Ala)$_n$.[13] If the resonance involves the fundamental and the overtone of the E_1 species amide II mode,[13] then the fundamental is expected at $3301 - (2 \times 1550 - 3067) = 3268$ cm^{-1}. Even allowing

TABLE I
Observed and Calculated Frequencies (in cm^{-1}) of α-Poly(L-Glutamic Acid)

Observed[a]		Calculated			
Raman[b]	ir	A	E_1	E_2	Potential Energy Distribution[c]
	3301VS[d]	3279			NH s(98)
			3279		NH s(98)
				3279	NH s(98)
		2982			C$^\gamma$H$_2$ as(99)
			2981		C$^\gamma$H$_2$ as(99)
				2981	C$^\gamma$H$_2$ as(99)
~2933VS	2939M	2943			C$^\gamma$H$_2$ ss(99)
			2943		C$^\gamma$H$_2$ ss(99)
				2943	C$^\gamma$H$_2$ ss(99)
		2918			C$^\beta$H$_2$ as(98)

TABLE I (*Continued*)
Observed and Calculated Frequencies (in cm⁻¹) of α-Poly(L-Glutamic Acid)

Observed[a]		Calculated			
Raman[b]	ir	A	E_1	E_2	Potential Energy Distribution[c]
			2918		$C^\beta H_2$ as(98)
				2918	$C^\beta H_2$ as(98)
~2883W	~2880 sh	{ 2884			$C^\alpha H^\alpha$ s(98)
			2884		$C^\alpha H^\alpha$ s(98)
				2884	$C^\alpha H^\alpha$ s(98)
		2855			$C^\beta H_2$ ss(98)
			2855		$C^\beta H_2$ ss(98)
				2855	$C^\beta H_2$ ss(98)
1720[e]	1718S[e]				$\nu(C^\delta = O)$ [1739(B_u)]
	1653VS‖[f]	1657			CO s(82),CN s(10),C^αCN d(10)
1652S			1655		CO s(82),CN s(11),C^αCN d(10)
				1645	CO s(83),CN s(12),C^αCN d(10)
		1561			$C^\delta O_2$ as(103)
			1561		$C^\delta O_2$ as(103)
				1561	$C^\alpha O_2$ as(103)
				1539	NH ib(46),CN s(31),CO ib(12), C^αC s(11)
	1550S⊥		1537		NH ib(46),CN s(33),CO ib(11), C^αC s(10)
	1510W‖[g]	1517			NH ib(46),CN s(35),CO ib(11)
				1459	$C^\beta H_2$ b(52),$C^\gamma H_2$ b(44)
1450M	1451W⊥		1459		$C^\beta H_2$ b(51),$C^\gamma H_2$ b(45)
		1458			$C^\beta H_2$ b(50),$C^\gamma H_2$ b(47)
1420M	1417M‖,⊥	{ 1445			$C^\gamma H_2$ b(48),$C^\beta H_2$ b(41)
			1445		$C^\gamma H_2$ b(49),$C^\beta H_2$ b(39)
				1445	$C^\gamma H_2$ b(51),$C^\beta H_2$ b(37)
		1416			$C^\delta O_2$ ss(67),$C^\alpha O_2$ b(24),$C^\gamma C^\delta$ s(15)
			1416		$C^\delta O_2$ ss(67),$C^\delta O_2$ b(24),$C^\gamma C^\delta$ s(15)
				1416	$C^\delta O_2$ ss(67),$C^\delta O_2$ b(24),$C^\gamma C^\delta$ s(15)
				1383	$C^\beta H_2$ w(35),H^α b1(25),$C^\alpha C^\beta$ s(13), $C^\beta C^\gamma$ s(12)
	1388W		1380		$C^\beta H_2$ w(36),H^α b1(22),$C^\beta C^\gamma$ s(13)
		1375			$C^\beta H_2$ w(41),H^α b1(18),$C^\beta C^\gamma$ s(15), $C^\alpha C^\beta$ s(12)
		1343			$C^\beta H_2$ tw(32),H^α b2(29)
			1341		$C^\beta H_2$ tw(33),H^α b2(20),$C^\gamma H_2$ tw(10)
				1339	$C^\beta H_2$ tw(41),$C^\gamma H_2$ tw(13),H^α b2(10)
1340M	1343 sh		1326		$C^\gamma H_2$ w(20),H^α b2(16),NH ib(11), $C^\beta H_2$ tw(10)
				1326	$C^\gamma H_2$ w(23),NH ib(19),C^αC s(12)
			1324		H^α b2(26),$C^\gamma H_2$ w(18),$C^\beta H_2$ tw(11)
				1311	H^α b2(47),$C^\gamma H_2$ w(21)
			1307		$C^\gamma H_2$ w(26),H^α b2(20),H^α b1(16), $C^\gamma H_2$ tw(13)
~1310W,br	1313W	{ 1305			$C^\gamma H_2$ w(30),H^α b1(21),$C^\gamma H_2$ tw(20)
1296M				1299	H^α b2(24),$C^\gamma H_2$ tw(23),NH ib(15)
	1283W⊥		1287		H^α b2(29),NH ib(25),$C^\gamma H_2$ tw(11)
				1263	NH ib(37),H^α b2(23),CN s(10), CO ib(10)

TABLE I (*Continued*)

Observed and Calculated Frequencies (in cm^{-1}) of α-Poly(L-Glutamic Acid)

Observed[a]		Calculated			
Raman[b]	ir	A	E_1	E_2	Potential Energy Distribution[c]
	1253MS[d]				ν(C—O) [1255(A_g)]
1214W	1212W$_{\parallel,\perp}$	1239			$C^\beta H_2$ w(37),$C^\gamma H_2$ w(20),H^α b2(10), $C^\gamma H_2$ tw(10)
			1237		$C^\beta H_2$ w(43),$C^\gamma H_2$ w(23)
				1236	$C^\beta H_2$ w(45),$C^\gamma H_2$ w(25)
		1173			H^α b1(35),$C^\beta H_2$ tw(22),$C^\gamma H_2$ tw(19)
1178W	1181W$_\perp$		1166		H^α b1(29),$C^\beta H_2$ tw(28),$C^\gamma H_2$ tw(28)
				1164	$C^\gamma H_2$ tw(33),$C^\beta H_2$ tw(31),H^α b1(25)
1117W	1118M$_{\parallel,\perp}$	1129			NC^α s(31),$C^\alpha C^\beta$ s(20),$C^\gamma H_2$ tw(16)
			1129		$C^\alpha C^\beta$ s(29),NC^α s(28)
				1127	$C^\alpha C^\beta$ s(35),NC^α s(25),H^α b1(11)
1080M	1083W$_\parallel$	1085			$C^\alpha C^\beta$ s(46)
			1079		$C^\alpha C^\beta$ s(30)
				1075	$C^\alpha C^\beta$ s(21),$C^\beta C^\gamma$ s(11),$C^\beta H_2$ (10)
				1048	$C^\beta C^\gamma$ s(48)
1057M	1060W$_{\parallel,\perp}$	1047	1048		$C^\beta C^\gamma$ s(50)
					$C^\beta C^\gamma$ s(51)
1030W	1028W				?
1002W				998	$C^\gamma C^\delta$ s(26),$C^\beta C^\gamma$ s(10),$C^\alpha C^\beta C^\gamma$ d(10)
	982W		996		$C^\gamma C^\delta$ s(28),$C^\beta C^\gamma$ s(10)
		992			$C^\gamma C^\delta$ s(33),$C^\beta C^\gamma$ s(10),$C^\delta O_2$ ss(10)
		975			$C^\gamma H_2$ r(28),NC^α s(18),$C^\beta H_2$ tw(12), $C^\beta H_2$ r(11),$C^\alpha C$ s(10)
			972		$C^\gamma H_2$ r(26),NC^α s(14),$C^\beta H_2$ tw(11), $C^\beta H_2$ r(11)
				969	$C^\gamma H_2$ r(26),NC^α s(14),$C^\beta H_2$ tw(11), $C^\beta H_2$ r(10)
				934	CN s(21),$C^\alpha C$ s(17)
	928W br		929		CN s(23),$C^\alpha C$ s(13)
924VS		922			CN s(27),CNC^α d(12)
	896W[e] }				ν(C^γ—COOH) [898(A_g),860(B_u)]
874W[e]	869W[e] }				
826W	~824MW		812		$C^\beta H_2$ r(34),$C^\gamma H_2$ r(24)
	~810MW	810			$C^\beta H_2$ r(38),$C^\gamma H_2$ r(27)
				807	$C^\beta H_2$ r(46),$C^\gamma H_2$ r(30)
	768VW		783		CO ob(25),$C^\beta H_2$ r(19)
		777			$C^\beta H_2$ r(13),$C^\delta O_2$ b(12),C^β b1(10)
				767	CO ob(46)
		746			CO ob(35),CN t(31)
			725		$C^\delta O_2$ b(38),$C^\delta O_2$ ss(12)
				720	$C^\delta O_2$ b(44),$C^\delta O_2$ ss(14)
	705W	706			$C^\delta O_2$ b(24),$NC^\alpha C$ d(15),$C^\delta O_2$ w(12), $C^\alpha CN$ d(11),$C^\beta C^\gamma C^\delta$ d(11)
				694	CO ib(18),CN t(14)
	~670MW		678		CN t(19),$NC^\alpha C$ d(12),NH ob(11)
				643	CN t(77),NH ob(44), NH $\cdots$ O ib(14)
		628			$C^\delta O_2$ w(26),$C^\delta O_2$ b20),CN t(20), $C^\gamma C^\delta$ s(10)

TABLE I (Continued)
Observed and Calculated Frequencies (in cm^{-1}) of α-Poly(L-Glutamic Acid)

Observed[a]		Calculated			
Raman[b]	ir	A	E$_1$	E$_2$	Potential Energy Distribution[c]
	618MW		626		CN t(42),$C^\delta O_2$ w(19),NH ob(17), $C^\delta O_2$ b(10)
				612	$C^\delta O_2$ w(46),$C^\delta O_2$ b(13)
			608		$C^\delta O_2$ w(26),CN t(21),NH ob(14), CO ob(12)
		581			$C^\delta O_2$ w(31),CN t(29),NH ob(25), CO ob(24)
562W	567W	549			C^αCN d(23),CN t(22),CO ib(21), NH ob(18),C^β b2(17),CO ob(12)
			515		NC^αC d(23),C^αCN d(13)
				500	$C^\delta O_2$ r(89)
		498			$C^\delta O_2$ r(88)
			498		$C^\delta O_2$ r(83)
495W				484	NC^αC d(30),CO ib(14),$C^\delta O_2$ w(12), C^αC s(11)
	475W[e]				δ(OC$^\delta$O) [478(B$_u$)]
	409M		402		CO ib(15),NH ob(15),CNC^α d(13), C^αCN d(10),CO ob(10)
385W				379	C^β b1(20),C^β b2(13),$C^\alpha C^\beta C^\gamma$ d(13), CNC^α d(12)
		368			CO ob(17),C^β b1(14),NC^αC d(11), $C^\beta C^\gamma C^\delta$ d(10),NH ob(10)
				353	C^β b2(31),C^αCN d(19)
			334		C^β b2(46),CO ib(11)
318W		334			CO ib(27),C^β b2(14),CNC^α d(10), $C^\alpha C^\beta C^\gamma$ d(10)
280VW		265			C^β b2(31),C^β b1(13)
			240		$C^\alpha C^\beta C^\gamma$ d(28), C^β b1(18), $C^\beta C^\gamma C^\delta$ d(12)
				234	$C^\alpha C^\beta C^\gamma$ d(38),C^β b1(15),CO ob(10)
				219	$C^\beta C^\gamma C^\delta$ d(22),C^αCN d(14),C^β 2(10)
			206		$C^\beta C^\gamma C^\delta$ d(15),$C^\alpha C^\beta C^\gamma$ d(13), C^αCN d(10)
204VW		{ 194			$C^\alpha C^\beta C^\gamma$ d(38),C^αCN d(14)
			175		CNC^α d(29),C^αCN d(14), $C^\beta C^\gamma C^\delta$ d(14),NH ob(11)
				171	NH ob(32),C^αCN d(18),CNC^α d(15), $C^\beta C^\gamma C^\delta$ d(13),C^β b2(11)
		170			$C^\beta C^\gamma C^\delta$ d(29),CNC^α d(25)
		130			$C^\gamma C^\delta$ t(41),$C^\alpha C^\beta$ t(12)
				121	$C^\gamma C^\delta$ t(53),$C^\alpha C^\beta$ t(12)
			117		$C^\gamma C^\delta$ (40)
		115			$C^\gamma C^\delta$ t(24)
				109	C^β b1(19),CNC^α d(11),$C^\beta C^\gamma C^\delta$ d(10)
		101			$C^\gamma C^\delta$ t(26),CN t(10),H$\cdots$O s(10)
				66	NH ob(20),NC^αC d(15),$C^\beta C^\gamma$ t(14), H$\cdots$O s(13)
			64		NH ob(25),NC^αC d(14),CN t(14), $C^\beta C^\gamma$ t(12)

TABLE I (*Continued*)
Observed and Calculated Frequencies (in cm^{-1}) of α-Poly(L-Glutamic Acid)

Observed[a]		Calculated			
Raman[b]	ir	A	E_1	E_2	Potential Energy Distribution[c]
		60			NC$^\alpha$ t(15),NC$^\alpha$C d(14),C$^\alpha$C t(14), C$^\alpha$C$^\beta$C$^\gamma$ d(12),CN t(12)
				39	NH ob(37),C$^\beta$ b1(19),C$^\alpha$C t(19), CN t(16),NC$^\alpha$ t(15),H $\cdots$ O s(10)
		35			C$^\alpha$C$^\beta$ t(45),C$^\beta$C$^\gamma$ t(37),C$^\gamma$C$^\delta$ t(11)
			35		C$^\alpha$C$^\beta$ t(51),C$^\beta$C$^\gamma$ t(29),C$^\gamma$C$^\delta$ t(12)
				35	C$^\alpha$C$^\beta$ t(46),C$^\beta$C$^\gamma$ t(31),C$^\gamma$C$^\delta$ t(12)
			23		C$^\beta$C$^\gamma$ t(32),C$^\alpha$C$^\beta$ t(14)
		21			C$^\beta$C$^\gamma$ t(42),C$^\alpha$C$^\beta$ t(28)
				21	C$^\beta$C$^\gamma$ t(28),NH ob(18),C$^\alpha$C$^\beta$ t(14), NC$^\alpha$C d(10)
			13		NH ob(39),C$^\beta$ b1(12),C$^\beta$C$^\gamma$ t(12), C$^\alpha$C$^\beta$ t(11),NC$^\alpha$C d(11)
				11	C$^\alpha$C t(36),H $\cdots$ O s(18)

[a] S = strong, M = medium, W = weak, V = very, sh = shoulder.

[b] From Ref. 8.

[c] s = stretch, as = antisymmetric stretch, ss = symmetric stretch, b = angle bend, ib = in-plane angle bend, ob = out-of-plane angle bend, w = wag, r = rock, tw = twist, d = deformation, t = torsion. Only contributions of 10% or greater are included.

[d] Observed frequency, not corrected for Fermi resonance.

[e] Modes primarily due to vibrations of the COOH group. In the PED column, we indicate the coordinate having the maximum contribution and the observed frequency in the acetic acid dimer (Ref. 14).

[f] Dichroism data from Refs. 3–5.

[g] From Refs. 3 and 7.

for anharmonicity effects,[13] this frequency is still about 7 cm^{-1} lower than the value of 3279 cm^{-1} found for the unperturbed NH stretch mode in α-(Ala)$_n$.[13] A possible explanation is that the hydrogen bond in α(GluH)$_n$ is slightly stronger than that in α-(Ala)$_n$.

The Raman and ir bands near 1720 cm^{-1} are clearly assignable to the hydrogen-bonded C=O stretch in the COOH group: the comparable band in the acetic acid dimer is at 1739 cm^{-1}.[14] The slight parallel dichroism of this band[3,5] indicates that the orientations of the COOH groups are such that (assuming uniaxial orientation) the C=O bonds make an angle of slightly less than 54.7° with the helix axis.[15] In view of the large dichroism of the amide I and amide II modes (see below), it is unlikely that the C=O bonds are oriented as nearly parallel to the helix axis as is required by the model in which side-chain COOH groups form a hydrogen-bonded helix.[16] In fact, in the solid state it is quite possible that interhelix COOH hydrogen bonds occur, perhaps in addition to intrahelix hydrogen bonds.

The A species amide I mode (primarily C=O stretch) is observed as a highly parallel dichroic[3-5] band at 1652 R, 1653 ir cm^{-1}, compared

with 1655 R, 1658 ir cm^{-1} in α-(Ala)$_n$.[12] The E_1 species amide II mode (primarily NH in-plane bend plus CN stretch) is found with high perpendicular dichroism[3-5] at 1550 cm^{-1} in the ir, compared with 1545 cm^{-1} in α-(Ala)$_n$.[12] Both of these small shifts in frequency in α-(GluH)$_n$ compared to α-(Ala)$_n$ are also consistent with a slightly stronger hydrogen bond in the former case and, taken together with the evidence from NH stretch, strongly support this possibility. The weak band observed at 1510 cm^{-1}, and having parallel dichroism,[3,5] is reasonably accounted for by the A species amide II mode calculated at 1517 cm^{-1}. (Note that predicted bands at 1561 cm^{-1} are a result of the assumption of a COO$^-$ group, which of course is not present. The COOH group that is present in α-(GluH)$_n$ is responsible for the 1720 cm^{-1} band discussed above.)

The observed bands at 1450 R, 1451 ir and 1420 R, 1417 ir cm^{-1} are well assigned to side-chain CH$_2$ bend modes. In aqueous solution at low pH, where (GluH)$_n$ is in an α-helix conformation, the Raman bands shift down to 1440 and 1412 cm^{-1}.[6] This may indicate that the side-chain conformation is different in the two cases, being not as fully extended in aqueous solution. We will examine other arguments pointing to this conclusion when we discuss the skeletal modes. (Note that predicted bands at 1416 cm^{-1} are a result of the assumption of a COO$^-$ group. The Raman spectrum at high pH, where the carboxyl groups are ionized, in fact shows a strong band at 1404 cm^{-1}.[6])

The $\sim$1400–1200 cm^{-1} region is one in which side-chain modes significantly influence main-chain modes. This mixing is much greater than in the case of α-(Ala)$_n$, where, for example, the CH$_3$ modes are completely separable from the amide III modes,[12] a situation that is not true for α-(GluH)$_n$. Nevertheless, the normal mode calculation gives good predictions of the observed bands. The weak ir band at 1388 cm^{-1} is reasonably assigned to A or E_1 species modes (the observed dichroism[3,5] is uncertain) that involve mixing of C$^\beta$H$_2$ wag with H$^\alpha$ bend. The 1340 cm^{-1} Raman band (with a weak counterpart in the ir at 1343 cm^{-1}) is observed to weaken slightly on N-deuteration.[8,11] The calculations predict that E_1 and E_2 modes at 1326 cm^{-1} contain NH in-plane bend contributions, while C$^\beta$H$_2$ twist plus H$^\alpha$ bend modes are predicted at 1343 and 1341 cm^{-1}. It is possible that the observed band at 1340 cm^{-1} contains an overlap of these two kinds of modes, thus weakening only partially on N-deuteration. A similar explanation was suggested for the 1336 cm^{-1} band of α-poly(γ-benzyl-L-glutamate).[17] The weak ir band at 1313 cm^{-1} appears to be unaffected by N-deuteration and is well assigned to C$^\gamma$H$_2$ wag modes at 1307(E_1) and 1305(A) cm^{-1} (the observed dichroism is uncertain). On the other hand, the Raman band at 1296 cm^{-1} clearly weakens on N-deuteration,[8] as does our observed ir band at 1283 cm^{-1}, and these are very well accounted for by the calculated modes at 1299(E_2) and 1287(E_1) cm^{-1}, respectively, that contain NH in-plane bend. (It is interesting to note that the com-

parable bands in α-(Ala)$_n$ are observed at 1278 R and 1270 ir cm^{-1} and are calculated at 1287(E$_2$) and 1278(E$_1$) cm^{-1}, respectively,[12] clearly showing the influence of the side-chain structure on the main-chain amide III modes.) The 1253 cm^{-1} ir band shows no conspicuous change in N-deuteration; therefore, it is unlikely to be an amide III mode, as previously suggested.[6] It is more likely to be due to C–O stretch in the COOH group, which is found at 1255 cm^{-1} in the acetic acid dimer.[14] The weak 1214 R, 1212 ir cm^{-1} bands are assignable to CH$_2$ wag modes, despite the large discrepancy with the predicted frequencies near 1238 cm^{-1}. This suggests that the $\sim$1238 cm^{-1} Raman band observed in α-(GluH)$_n$ at low pH[6] should be assigned to CH$_2$ wag and not amide III, as proposed.[6] The 1178 R, 1181 ir cm^{-1} bands are reasonably well predicted and arise from H$^\alpha$ bend plus C$^\beta$H$_2$ twist modes.

The $\sim$1100–900 cm^{-1} region is dominated by main-chain and side-chain backbone stretching vibrations. The bands in this region are not only well predicted by the calculation, but the differences, as compared with β-(GluCa)$_n$ and α-(Ala)$_n$, are also accounted for. in α-(GluH)$_n$, the 1117 R, 1118 ir cm^{-1} bands are due to mixed NC$^\alpha$ stretch and C$^\alpha$C$^\beta$ stretch modes calculated at 1129 cm^{-1}. The same mixing occurs in β-(GluCa)$_n$, but the C$^\alpha$C$^\beta$ stretch predomininates[1] and the mode is calculated at 1111 cm^{-1} but seems not to be observed. In α-(Ala)$_n$, NC$^\alpha$ stretch mixes with CH$_3$ rock and C$^\alpha$C$^\gamma$ stretch,[12] with the result that the calculated and observed frequencies are near 1170 cm^{-1}. The 1080 R, 1083 ir cm^{-1} bands of α-(GluH)$_n$ are associated with a mainly C$^\alpha$C$^\beta$ stretch mode calculated at 1085(A) cm^{-1}. In β-(GluCa)$_n$, this mode is significantly mixed with C$^\beta$C$^\alpha$ stretch,[1] being calculated at 1062(A) cm^{-1} and observed at 1066 cm^{-1}. In α-(Ala)$_n$, this mode is mixed with CH$_3$ rock[12] and is calcualted at 1103 and observed near 1107 cm^{-1}. Similarly, the 1057 R, 1060 ir cm^{-1} bands of α-(GluH)$_n$ are due mainly to C$^\beta$C$^\gamma$ stretch modes calculated near 1048 cm^{-1}, which give rise to a medium-intensity Raman band. In β-(GluCa)$_n$, this mode mixes with C$^\alpha$C$^\beta$ stretch and C$^\beta$H$_2$ rock, calculated at 1041 cm^{-1}, and gives rise to a very weak Raman band at 1050 cm^{-1}. The observed bands at 1002 R, 982 ir cm^{-1} are associated with mixed C$^\gamma$C$^\delta$ and C$^\beta$C$^\gamma$ stretch, with calculated frequencies at 998(E$_2$) and 996(E$_1$), 992(A) cm^{-1}; in β-(GluCa)$_n$, the C$^\gamma$C$^\delta$ stretch is relatively unmixed[1] and seems to be associated with calculated and observed frequencies at 1003 and $\sim$1013 cm^{-1}, respectively. The calculations do not predict additional modes to which the weak Raman and ir bands near 1030 cm^{-1} could be assigned. The Raman spectrum of α-(GluMg)$_n$ shows only a shoulder near this frequency whereas there is a pronounced band in α-(GluCa)$_n$.[11] It seems quite possible that such a band is associated with a side chain that is not fully extended. This band also is present in the Raman spectrum of α-(GluH)$_n$ in aqueous solution at low pH,[6] where we have seen that shifted CH$_2$ bend frequencies also indicate a possible departure from a fully extended side chain. A strong Raman

band in the 1000–900 cm^{-1} region is usually considered to be characteristic of the α-helix structure.[18] Such a band is found in α-(GluH)$_n$ at 924 cm^{-1}, in excellent agreement with the calculated mode at 922 cm^{-1}. Note that this mode, with contributions in addition to CN stretch and CNC$^\alpha$ deformation, is predicted at 910 cm^{-1} in α-(Ala)$_n$,[12] and is, indeed, found at a lower frequency, viz., 908 cm^{-1}.

The 896 ir and 874 R, 869 ir cm^{-1} bands can be correlated with CC stretch modes found in the acetic acid dimer.[14] These, of course, correspond to our C$^\gamma$C$^\delta$ stretch, but the contribution of the latter may be modified by our assumption of a terminal COO$^-$ group. The 826 R, 824 ir and the 810 ir cm^{-1} bands can be assigned to predicted CH$_2$ rock modes. Since the calculations do not predict a large splitting, it is possible that one of the above bands (probably near 825 cm^{-1}) could be associated with modes of a disordered side chain. In α-(Ala)$_n$, a medium intensity ir band at 774 cm^{-1} is assignable to an E$_1$ species C=O out-of-plane bend mode calculated at 780 cm^{-1} [12]; we assign the 768 ir cm^{-1} band of α-(GluH)$_n$ by analogy (although it may also be correlated with the 777 cm^{-1} A species mode). Similarly, in α-(Ala)$_n$ a band at 693 R, 691 ir cm^{-1} is assignable to a NC$^\alpha$C plus C$^\alpha$CN deformation mode calculated at[12] 700(A) cm^{-1}; it seems reasonable to assign the 705 cm^{-1} band of α-(GluH)$_n$ analogously (although there are some "fictitious" contributions of C$^\delta$O$_2$ bend and wag to the calculated 706 cm^{-1} mode).

The amide V modes (NH out-of-plane bend plus CN torsion) of α-(Ala)$_n$ are calculated at 660(E$_1$) and 608(E$_1$) cm^{-1}, and they are observed as strong bands in the ir at 658 and 618 cm^{-1}, respectively.[12] In α-(GluH)$_n$, these modes are calculated at 678 and 626 cm^{-1}, and it seems reasonable to assign ir bands at 670 and 618 cm^{-1}, respectively, to these modes. (It should be noted that the former band in not to be confused with a carbon dioxide band that occurs near this frequency, and whose small residual appearance has been subtracted out.) While the 618 cm^{-1} band clearly weakens on N-deuteration, consistent with this assignment, it seems as if this is not the case for the 670 cm^{-1} band. This apparent discrepancy, in fact, demonstrates the importance of normal mode calculations in a complete analysis. We have computed the normal modes of the N-deuterated molecule and find an interesting feature in the 700–600-cm^{-1} region for the E$_1$ species: a band is predicted at 662 cm^{-1}, having a PED of CO ob(16) NC$^\alpha$C d(13) CO ib(13) C$^\delta$O$_2$ w(12). (There is also a predicted mode at 613 cm^{-1} that is mainly C$^\delta$O$_2$ wag, as is the case for the 608 cm^{-1} mode of the protonated molecule.) This is somewhat analogous to the situation in α- (AlaND)$_n$, where a mode with a similar PED is predicted at 632(E$_1$) and observed at 647 ir cm^{-1}.[12] In the latter case, there is no overlap with either amide V mode of the protonated molecule, but for α-(GluH)$_n$ such an overlap is indicated and probably accounts for the apparent lack of intensity decrease near 670 cm^{-1} on N-deuteration. The amide V' mode

is predicted at $466(E_1)$ cm^{-1}, and we suppose that the increased intensity in the N-deuterated molecule at 475 cm^{-1} (where a bending vibration of the COOH group occurs) is due to the additional contribution from ND out-of-plane bend.

Special features of the α-(GluH)$_n$ spectrum in the lower frequency region are also predicted reasonably well by the calculation. The 562 R, 567 ir cm^{-1} band is assignable to a highly mixed mode including an NH out-of-plane bend calculated at 549(A) cm^{-1}. A mode of similar character is calculated at 537(A) cm^{-1} in α-(Ala)$_n$,[12] and it has an observed counterpart at 530 R, 526 ir cm^{-1}. The ir band at 409 cm^{-1} is uniquely assignable to the calculated $402(E_1)$ cm^{-1} mode of mixed character that also includes an NH out-of-plane bend. [A similar band is found in α-helical polyglutamate esters,[19] such as poly(γ-methyl-L-glutamate (410 cm^{-1}), poly(γ-benzyl-L-glutamate (408 cm^{-1}), and poly(γ-ethyl-L-glutamate) (405 cm^{-1}).] A mode of almost identical character is calculated at $374(E_1)$ cm^{-1} in α-(Ala)$_n$,[12] and it is observed at 375 R, ir cm^{-1}. It is interesting that, although both modes contain a similar C^β bend 2 contribution, and other side-chain contributions in α-(GluH)$_n$ are below the 10% PED level [$C^\alpha C^\beta C^\gamma$ d(9) C^β bl(7) $C^\beta C^\gamma C^\delta$ d(6)], the frequencies are so different and this difference is so well accounted for. This testifies to the high reliability of the force field.

CONCLUSIONS

The normal modes of α-(GluH)$_n$ have been calculated using the same helix structure and force field as for α-(Ala)$_n$[12] and a force field for an extended side chain transferred from β-(GluCa)$_n$.[1] Despite an indication of a slightly stronger hydrogen bond in α-(GluH)$_n$ than in α-(Ala)$_n$, and therefore the possibility that a force field refined for the latter would not be completely satisfactory for predicting normal modes of the former, the observed Raman and ir bands are in general accounted for quite well. This indicates that the force field is highly reliable and transferable. In many cases, particularly in the amide III and 1100–900 cm^{-1} backbone stretching regions, significant differences are predicted and observed between the spectra of α-(GluH)$_n$ and α-(Ala)$_n$, thus clearly demonstrating the influence of the side chain on the vibrations of the main chain.

References

1. Sengupta, P. K. & Krimm, S. (1984) *Biopolymers* **23**, 1565–1594.
2. Krimm, S. (1983) *Biopolymers* **22**, 217–225.
3. Ambrose, E. M. (1950) *J. Chem. Soc.* 3239–3249 (appendix to W. E. Hanby, S. G. Waley & J. Watson).
4. Blout, E. R. & Idelson, M. (1956) *J. Am. Chem. Soc.* **78**, 497–498.

5. Lenormant, H., Baudras, A. & Blout, E. R. (1958) *J. Am. Chem. Soc.* **80**, 6191–6195.

6. Koenig, J. L. & Frushour, B. (1972) *Biopolymers* **11**, 1871–1892.

7. Miyazawa, T. & Blout, E. R. (1961) *J. Am. Chem. Soc.* **83**, 712–719.

8. Fasman, G. D., Itoh, K., Liu, C. S. & Lord, R. C. (1978) *Biopolymers* **17**, 1729–1746.

9. Doty, P., Wada, A., Yang, J. T. & Blout, E. R. (1957) *J. Polym. Sci.* **23**, 851–861.

10. Zimmerman, S. S. & Mandelkern, L. (1975) *Biopolymers* **14**, 567–584.

11. Sengupta, P. K. & Krimm, S. (1985) *Spectrochim. Acta* **41A**, 205–207.

12. Dwivedi, A. M. & Krimm, S. (1984) *Biopolymers* **23**, 923–943.

13. Krimm, S. & Dwivedi, A. M. (1982) *J. Raman Spectrosc.* **12**, 133–137.

14. Nakamoto, K. & Kishida, S. (1964) *J. Chem. Phys.* **41**, 1558–1563.

15. Fraser, R. D. B. (1953) *J. Chem. Phys.* **21**, 1511–1515.

16. Fasman, G. D. (1967) in *Poly-α-Amino Acids*, Fasman, G. D., Ed., Dekker, New York, p. 499.

17. Koenig, J. L. & Sutton, P. L. (1971) *Biopolymers* **10**, 89–106.

18. Frushour, B. G. & Koenig, J. L. (1975) in *Advances in Infrared and Raman Spectroscopy*, Vol. 1, Heyden, London, pp. 35–97.

19. Miyazawa, T., Fukushima, K. & Sugano, S. (1967) in *Conformation of Biopolymers*, Vol. 2, Ramachandran, G. N., Ed., Academic, New York, pp. 557–568.